Physica B 514 (2017) 89–95

Contents lists available at ScienceDirect

Physica B

journal homepage: www.elsevier.com/locate/physb

Enhanced superconductivity and superconductor to insulator transition in nano-crystalline molybdenum thin films

Shilpam Sharma[a], E.P. Amaladass[a], Neha Sharma[b], V. Harimohan[a], S. Amirthapandian[c], Awadhesh Mani[a,*]

[a] Condensed Matter Physics Division, Materials Science Group, Indira Gandhi Centre for Atomic Research, Kalpakkam 603102, India
[b] Surface & Nanoscience Division, Materials Science Group, Indira Gandhi Centre for Atomic Research, Kalpakkam 603102, India
[c] Materials Physics Division, Materials Science Group, Indira Gandhi Centre for Atomic Research, Kalpakkam 603102, India

ARTICLE INFO

Keywords:
Thin films (A)
Electron microscopy (C)
Superconductivity (D)
Transport properties (D)

ABSTRACT

Disorder driven superconductor to insulator transition via intermediate metallic regime is reported in nano-crystalline thin films of molybdenum. The nano-structured thin films have been deposited at room temperature using DC magnetron sputtering at different argon pressures. The grain size has been tuned using deposition pressure as the sole control parameter. A variation of particle sizes, room temperature resistivity and superconducting transition has been studied as a function of deposition pressure. The nano-crystalline molybdenum thin films are found to have large carrier concentration but very low mobility and electronic mean free path. Hall and conductivity measurements have been used to understand the effect of disorder on the carrier density and mobilities. Ioffe-Regel parameter is shown to correlate with the continuous metal-insulator transition in our samples.

1. Introduction

Even though an old area of research in material science, the studies on the effect of disorder on normal and superconducting states of metallic superconductors still remains an open problem that is enjoying a renewed interest recently [1–11]. The disorder and superconductivity (SC) have contrasting effects on the electrical properties of material: while the former causes increase in the resistivity by localizing electron wave-functions, latter gives rise to zero resistivity on account of formation of long range ordered condensate in a macroscopic quantum state. Based on Bardeen-Cooper-Schrieffer (BCS) theory of *s*-wave superconductors, Anderson postulated that superconductivity in a metallic system can't be destroyed by weak or moderate disorder but grains ceases to be superconducting below a critical size (D_C), at which the superconducting gap equals the energy level spacing due to energy band discretization (Kubo gap) [12]. It was however, later observed that amorphous or granular thin film of many s-wave superconductors show a superconductor to insulator transition (SIT) initiated by a change of control parameter such as an increase in disorder [5,13–15] or application of parallel or perpendicular magnetic field [16–18].

SIT, occurring in amorphous or granular thin films is an example of continuous quantum phase transition that transforms a coherent superconducting state in to a localized insulating ground state across the phase boundary [19]. The transition from superconducting to insulating state, tuned by change of some control parameter, could be a continuous transition such as seen in ultrathin films of amorphous Bi [20] or there could appear an intermediate, quantum corrected localized metallic regime (M) like the S-M-I transition reported in Nb_xSi_{1-x} alloy films [14,21,22]. In the metallic regime of the split S-M-I transition, the conductivity extrapolates to a finite value at T=0 but the resistance remains much lower than that of the normal state [22]. The theoretical understanding of the SIT is based on mainly two models: the Bosonic model presumes that Cooper pairs exist in insulating state and transition occurs due to Bose-Einstein condensation [19,23] whereas, the Fermionic model considers that in the dirty system at zero temperature, the electrons do not pair and normal Fermionic state electrons undergo Anderson localization [23].

In addition to occurrence of SIT, superconducting properties such as transition temperature (T_C), superconducting gap and upper critical field (H_{C2}) show strong dependence on the degree of disorder or size of the superconducting grains embedded in the amorphous material. Increasing disorder by reducing particle size is known to increase or decrease T_C depending upon the coupling strength and the smearing of density of states at the Fermi level [24,25]. Weakly coupled type I superconductors, such as Al, Sn, In, W and Re, show an increase in

* Corresponding author.
E-mail address: mani@igcar.gov.in (A. Mani).

http://dx.doi.org/10.1016/j.physb.2017.03.044
Received 8 November 2016; Received in revised form 24 March 2017; Accepted 27 March 2017
Available online 30 March 2017

their T_C in the disordered state [24,26,27]. Type II superconductor with intermediate coupling like Nb shows a decrease in the superconducting gap and T_C with reduction in particle size [28]. For strongly coupled Pb, while many reports on thin films exhibit no size dependent change in T_C [27], there are reports of reduction in T_C of Pb powder and thin films with grains below a critical size mainly due to discretization of electronic energy levels [29,30].

There are few reports of enhancement of T_C in thin amorphous films of Mo deposited at liquid helium temperature [31] but here we report disorder induced SIT via intermediary metallic phase in molybdenum thin films, sputter deposited at room temperature under varying argon pressure. In addition to transition into insulating state, our nano-crystalline thin films show enhancement in T_C as reported in amorphous Mo films [24]. Detailed structural characterization and analysis using high resolution transmission electron microscopy (HRTEM) have been performed to understand the effect of deposition pressure on the grain size and normal state resistivity. Effective disorder in these films has been characterized by the Ioffe-Regel parameter ($k_F l$) [32] (k_F is the Fermi wave vector and l_e is the electron mean free path). A striking correlation in deposition pressure, disorder and particle size with superconducting and normal state properties of the Mo films has been brought about from these analyses.

2. Experimental details

Nano-crystalline thin films of Mo were deposited on the cleaned glass substrates using a home built magnetron deposition system. Sputter deposition was carried out from a 99.97% pure Mo target using a custom built 1″ magnetron cathode. Deposition chamber can reach up to a base pressure of ~1×10^{-7} mbar and the oxygen partial pressure measured using residual gas analyzer was found to be less than 10^{-9} mbar. The average particle size in the Mo films was reproducibly controlled by varying Ar pressure in 13 μbar to 3 μbar range. Films were deposited with direct current fixed at 40 mA and voltage varying between 270 V and 325 V. Thickness measurements were performed using Dektak profilometer, Rutherford back scattering and X-ray reflectivity (XRR) measurements. As the films were found to be X-ray amorphous, phase and microstructure of the nano-crystalline films was characterized using transmission electron microscopy (TEM) on mechanically scratched films transferred onto carbon grid. High resolution TEM measurements were performed using LIBRA 200FE HRTEM operated at 200 keV, equipped with an in-column energy filter and Schottky field emission gun source. Electron diffraction patterns (SAED) and electron energy loss spectrums (EELS) were collected at different regions of the samples to confirm purity of Mo phase in the films. In-field transport measurements were performed using M/S cryogenic Inc. U.K. make cryogen free, 15 T magneto-transport cryostat capable of reaching temperatures as low as 1.8 K from 300 K. Hall and resistivity measurements were performed in Hall bar and Van der Pauw geometry respectively [33,34].

3. Results and discussion

All the nano-crystalline Mo films were deposited on glass substrates at different Ar pressures varying from 3 μbar to 13 μbar while maintaining same DC current of 40 mA. The thickness of all the films was found to be roughly 56 nm as measured using Rutherford backscattering, Dektak profilometer and XRR measurements.

To estimate film thickness and roughness, XRR data was fitted using Parratt32 routine [35]. A representative XRR data along with fit is presented in Fig. 1. The surface roughness of the films was found to be ~2.5 nm. These Mo thin films were characterized for phase and microstructure using HRTEM. Fig. 2(a)–(d) show the HRTEM images of the films deposited at different Ar pressures 3.0, 4.5, 7.0 and 13.0 μbar respectively. It can be clearly seen that the film deposited at 3 μbar has large particles with sharp particle boundaries and as the

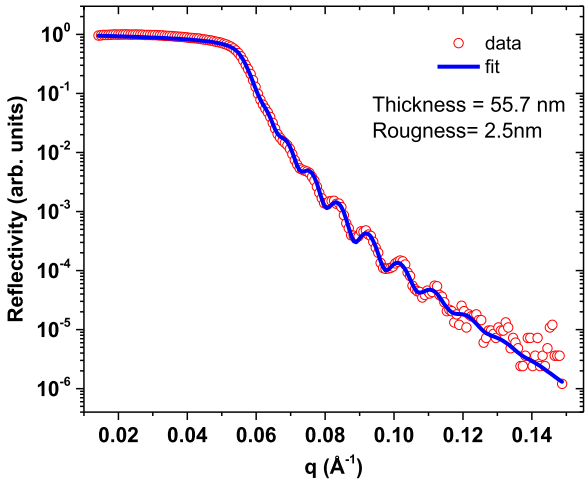

Fig. 1. X-ray reflectivity as a function of scattering vector. Thickness of the film was estimated by fitting the XRR data. A thickness of ~56 nm with a low surface roughness of ~2.5 nm has been observed.

deposition pressure increases, particle size reduces. In the HRTEM image (c.f. Fig. 2(e)) of sample deposited at 3 μbar Ar pressure, two grains can be identified with crystalline order ranging up to 5–6 nm with inter-granular region of roughly 2 nm. With increase in the deposition pressure, inter-granular region comprising of amorphous Mo with no long range order but some degree of short range order is seen to increase.

Fig. 2(a)–(d) also show corresponding SAED patterns collected from the samples. It can be observed from Fig. 2(a) that the film deposited at 3 μbar is polycrystalline in nature with well-defined Debye-Scherrer ring pattern. The ring pattern was analyzed using "process diffraction' software [36]. All the d-spacing in SAED pattern were indexed to BCC Mo with a lattice parameter ~2.9404 Å, smaller than the reported value of 3.1472 Å [37] thus indicating a compressive stress in the film. Similar changes in lattice parameters of nano-crystalline films of Nb and gold have already been reported in literature [28,38,39]. Other than BCC Mo d-spacings, the d-spacing corresponding to impurity phases like molybdenum oxide etc. have not been observed in the diffraction pattern. With increase in the deposition pressure, Debye-Scherrer rings in the SAED patterns (c.f. fig. 2b–d) can not be discerned and the patterns resemble diffraction pattern of amorphous material with diffused rings. For sample deposited at 4.5 μbar pressure (fig. 2(b)), a few crystalline spots can be observed on the amorphous electron diffraction pattern. Fig. 2(f) and (g) show dark field and bright field TEM micrographs for 7 μbar and 13 μbar deposited samples. Dark contrast due to diffracting grains can be observed. It can be seen that the number density of the particles is decreasing with increase in deposition pressure.

The particle size distribution of these films has been estimated by analyzing dark field TEM micrographs using ImageJ software [40]. The average particle size has been estimated by fitting log-normal distribution to the size distribution histograms of roughly 100–150 different particles. The particle size distribution along with representative dark field TEM micrographs is presented in Fig. 3. The average particle size decreases from 5.5 nm to 2.5 nm with increase in deposition pressure (P) from 3 μbar to 7 μbar. With a further increase of pressure from 7 μbar to 13 μbar, particle size does not decrease below ~2.5 nm, nonetheless, the average particle density decreases. The variation of average particle size with deposition pressure is presented in Fig. 4. It can be seen that particle size decreases rapidly as the pressure is increased from 3 μbar to 7 μbar and beyond P > 7 μbar it remains nearly constant at ~2.5 nm. A smaller than reported value of the lattice parameter of our films can thus be due to pressure from grain boundary on these small crystallites. Nano-structured Nb thin films